Light Z' Signatures at the LHC

Yaşar Hiçyılmaz[1,2], Shaaban Khalil[3] and Stefano Moretti[2,4]
[1]*Department of Physics, Balıkesir University, TR10145, Balıkesir, Turkey*
[2]*School of Physics and Astronomy, University of Southampton, Highfield, Southampton SO17 1BJ, United Kingdom*
[3]*Center for Fundamental Physics, Zewail City of Science and Technology, 6 October City, Giza 12588, Egypt*
[4]*Department of Physics & Astronomy, Uppsala University, Box 516, SE-751 20 Uppsala, Sweden*

(Dated: Tuesday 20th September, 2022)

We propose a theoretical framework embedding a spontaneously broken $U(1)'$ symmetry in addition to the Standard Model (SM) gauge group, from which a very light Z' state emerges, with both vector and axial (non-universal) couplings to fermions, able to explain the so-called Atomki anomaly, compliant with current measurements of the Anomalous Magnetic Moments (AMMs) of electron and muon as well as beam dump experiments while providing a distinctive $pp \to \text{Higgs} \to Z'Z' \to 4l$ ($l = e, \mu$) signal at the Large Hadron Collider (LHC), where the 'Higgs' label refers to the SM-like Higgs state discovered in 2012 or a lighter one. We finally show that the cross section for this process should be sufficiently large to afford one with significant sensitivity during Run 3 of the LHC.

A light neutral Z' boson (often dubbed a 'dark photon'), with mass of order 17 MeV, provides a natural explanation for the clear anomaly observed by the Atomki collaboration [1] in the decay of excited states of Beryllium [2–7]. Furthermore, several studies have been conducted to investigate the effects of such light Z' on the AMM of the electron (a_e) and muon (a_μ) as well as B anomalies such as $R_{K^{(*)}}$ [8–15].

In this letter we analyse some LHC signatures of a light Z' associated with a non-universal $U(1)'$ extension of the Standard Model (SM). This type of scenario has been shown to account for both the Atomki anomaly and $a_{e,\mu}$ results [16]. In addition, we revisit the contributions of such light Z' to these observables to see how the most recent experimental results constrain the associated couplings.

We focus on a non-universal $U(1)'$ extension of the SM in which the kinetic term in the Lagrangian is given by

$$\mathcal{L}_{\rm kin} = -\frac{1}{4}\hat{F}_{\mu\nu}\hat{F}^{\mu\nu} - \frac{1}{4}\hat{F}'_{\mu\nu}\hat{F}'^{\mu\nu} - \frac{\eta}{2}\hat{F}'_{\mu\nu}\hat{F}^{\mu\nu}, \quad (1)$$

where η quantifies the mixing between the SM $U(1)_Y$ and extra $U(1)'$. After the diagonalization of Eq. (1), the covariant derivative can be written as

$$\mathcal{D}_\mu = \partial_\mu + ... + ig_1 Y B_\mu + i(\tilde{g}Y + g'z)B'_\mu, \quad (2)$$

where Y and g_1 are the hypercharge and its gauge coupling while z and g' are the $U(1)'$ charge and its gauge coupling. Further, $\tilde{g}$ is the mixed gauge coupling between the two groups. The $U(1)'$ symmetry is broken by a new SM singlet scalar, χ, with $U(1)'$ charge z_χ and Vacuum Expectation Value (VEV) v'. The scalar potential for the Higgs fields can be written as

$$V(H,\chi) = -\mu^2|H|^2 + \lambda|H|^4 - \mu_\chi^2|\chi|^2 + \lambda_\chi|\chi|^4 + \kappa|\chi|^2|H|^2. \quad (3)$$

Here, H is the SM Higgs doublet while κ is the mixing parameter which connects that SM and χ Higgs fields. After Electro-Weak Symmetry Breaking (EWSB), for $\mu^2 = \lambda v^2 + \frac{1}{2}\kappa v'^2$ and $\mu_\chi^2 = \lambda_\chi v'^2 + \frac{1}{2}\kappa v^2$, the Higgs mass matrix in the (h_2, h_1) basis can be written as

$$m^2_{h_2 h_1} = \begin{pmatrix} 2\lambda v^2 & \kappa v v' \\ \kappa v v' & 2\lambda_\chi v'^2 \end{pmatrix}, \quad (4)$$

where h_2 is dominantly the SM-like Higgs boson while the exotic state h_1 is dominantly the singlet Higgs (χ-like). In this work, we consider $m_{h_1} < m_{h_2}$ and the $h_1 \to Z'Z'$ decay rate ≥ 0.95, which are be compatible with experimental results. The SM-like Higgs boson h_2 can decay to Z' pairs too, proportionally to κ. Moreover, the spontaneous breaking of the $U(1)'$ symmetry implies the existence of a mass term $m_{Z'} = g' z_\chi v'$. Thus, if $g' \sim \mathcal{O}(10^{-4} - 10^{-5})$, M'_Z would be of order $\mathcal{O}(10)$ MeV. It is worth noting that we adopt non-universal charge assignments of the SM particles under $U(1)'$, as discussed in Ref. [16]. These assignments satisfy anomaly cancellation conditions, enforcing a gauge invariant Yukawa sector of the third fermionic generation and family universality in the first two while not allowing coupling between Z' and light neutrinos.

The Neutral Current (NC) interactions of this additional vector boson with the SM fermions are given as

$$\mathcal{L}^{\rm Z'}_{\rm NC} = -\sum_f \bar{\psi}_f \gamma^\mu \left(C_{f,L}P_L + C_{f,R}P_R\right)\psi_f Z'_\mu, \quad (5)$$

where Left (L) and Right (R) handed coefficients are written as

$$C_{f,L} = -g_Z \sin\theta' \left(T^3_f - \sin^2\theta_W Q_f\right) + (\tilde{g}Y_{f,L} + g' z_{f,L})\cos\theta', \quad (6)$$

$$C_{f,R} = g_Z \sin^2(\theta_W)\sin(\theta')Q_f + (\tilde{g}Y_{f,R} + g' z_{f,R})\cos(\theta'). \quad (7)$$

The parameters given in these expressions can be found in Ref. [16].

The contribution of this Z' gauge boson to the AMMs of the charged leptons a_f, for $f = e, \mu, \tau$ is given by [17]

$$\Delta a_f = \frac{m_f^2}{4\pi^2 m_{Z'}^2}\Big(C_{f,V}^2 \int_0^1 \frac{x^2(1-x)}{1-x+x^2 m_\alpha^2/m_{Z'}^2}dx - C_{f,A}^2 \int_0^1 \frac{x(1-x)(4-x)+2x^3 m_f^2/m_{Z'}^2}{1-x+x^2 m_f^2/m_{Z'}^2}dx\Big), \quad (8)$$

where $C_{f,V} = \frac{C_{f,R}+C_{f,L}}{2}$ and $C_{f,A} = \frac{C_{f,R}-C_{f,L}}{2}$.

It is important to note that the contribution of the Z' to the AMMs of leptons is primarily determined by their vector and axial couplings as well as the mass of the Z' boson. Furthermore, the vector and axial couplings of the quarks are important in explaining the Atomki anomaly via the transition. $^8\text{Be}^* \to {}^8\text{Be}\, Z'$ [18]. In particular, the contribution of the quark axial couplings $C_{q,A}$ in this transition is greater than that of the vector couplings $C_{q,V}$ because the $C_{q,A}$ and $C_{q,V}$ terms are proportional to $k/M_{Z'}$ and $k^3/M_{Z'}^3$ (where k is the small momentum of the Z'), respectively [19].

Parameter	Scanned range	Parameter	Scanned range
g'	$[10^{-5}, 5\times 10^{-5}]$	λ	$[-0.132, -0.125]$
$\tilde{g}$	$[-10^{-3}, 10^{-3}]$	λ_χ	$[-10^{-5}, -10^{-3}]$
v_S	$[0.1, 1]$ TeV	κ	$[10^{-6}, 10^{-3}]$

TABLE I: *Scanned parameter space of our model.*

In our numerical analysis, we have employed SPheno 4.0.4 [20–22] generated with SARAH 4.14.3 [23, 24]. In Fig. 1, we show the portion of (g_p, $\tilde{g}$) parameter space that satisfies the current experimental bounds from $(g-2)_{e,\mu}$, the $^8\text{Be}^*$ anomaly and NA64 (as well as electron beam dump experiments) [25**?** – 27]. Here, the darkest shaded blue regions comply with all such constraints. During the scanning of the $U(1)'$ parameter space, within the ranges specified in Tab. I, the Metropolis-Hastings algorithm has been used. After data collection, we implement Higgs boson mass bounds [29, 30] as well as constraints from Branching Ratios (BRs) of B decays such as $\text{BR}(B \to X_s\gamma)$ [31], $\text{BR}(B_s \to \mu^+\mu^-)$ [32] and $\text{BR}(B_u \to \tau\nu_\tau)$ [33]. We have also bounded the Z/Z' mixing to be less than a few times 10^{-3} as a result of EW Precision Tests (EWPTs) [34].

The experimental constraints can be summarized as follows:

$$\begin{aligned}
&m_h = 122 - 128 \text{ GeV(as our masses are lowest order)},\\
&2.99\times 10^{-4} \le \text{BR}(B\to X_s\gamma) \le 3.87\times 10^{-4}\ (2\sigma \text{ tolerance}),\\
&0.15 \le \frac{\text{BR}(B_u\to\tau\nu_\tau)}{\text{BR}(B_u\to\tau\nu_\tau)_{\text{SM}}} \le 2.41\ (3\sigma \text{ tolerance}),\\
&\Delta a_e = (4.8 \pm 9.0)\times 10^{-13}\ (3\sigma \text{ tolerance}),\\
&\Delta a_\mu = (2.51 \pm 1.77)\times 10^{-9}\ (3\sigma \text{ tolerance}).
\end{aligned} \quad (9)$$

Additionally, the cross section values for the given processes at the LHC have been calculated by using CalcHEP [35].

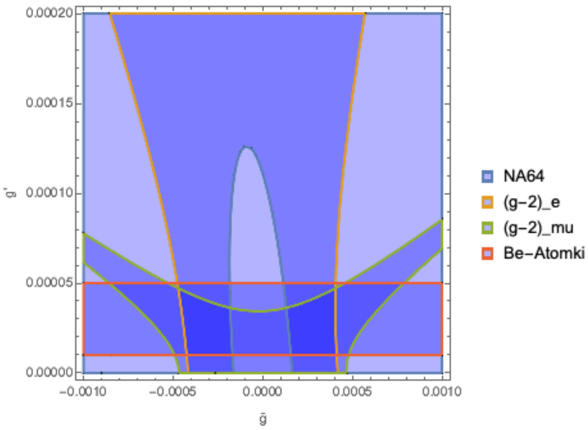

FIG. 1: Allowed parameter space mapped on the $(g', \tilde{g})$ plane for Z' mass of 17 MeV against four different experimental constraints.

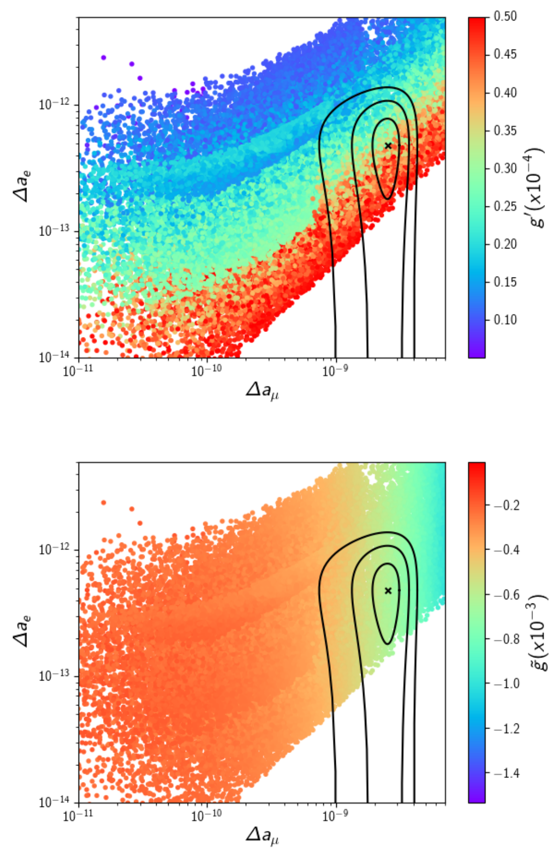

FIG. 2: Results for g' (top) and $\tilde{g}$ (bottom) in terms of $(g-2)_e$ vs $(g-2)_\mu$. Each solid line from inner to outer represents 1σ, 2σ and 3σ bounds from the experimental central values in Eq. (9).

I. RESULTS

In this section, we will first present the dependence of Δa_μ and Δa_e to the fundamental parameters g' and $\tilde{g}$. Fig. 2 depicts Δa_μ vs Δa_e. where the color bars show g' (top panel) and $\tilde{g}$ (bottom panel) parameters. Herein, one can learn about the favoured ranges of these parameters in order to obtain Am Ms within their 1σ, 2σ and 3σ value. As seen from the plots, the experimental bounds of Δa_μ and Δa_e within 3σ allow for a narrow range in $\tilde{g}$, namely, $-0.6 \times 10^{-3} \lesssim \tilde{g} \lesssim -0.4 \times 10^{-3}$ while g' lies in the range of $0.2 \times 10^{-4} \lesssim g' \lesssim 0.5 \times 10^{-4}$.

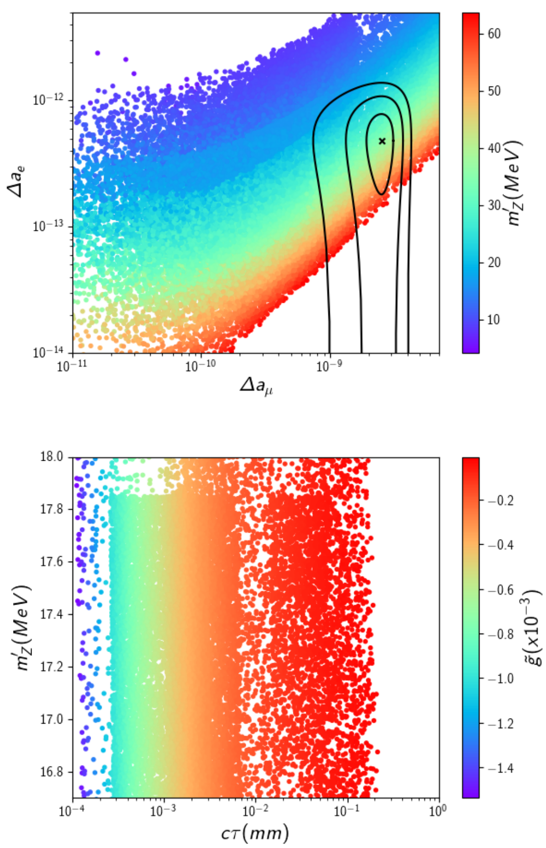

FIG. 3: Results for $m_{Z'}$ in terms of $(g-2)_e$ vs $(g-2)_\mu$ (top) and for $\tilde{g}$ in terms of $m_{Z'}$ vs the proper lifetime of the Z' (for $m_Z' \approx 17$ EV).

Now, let us focus on Z' properties, such as its mass $m_{Z'}$ and proper lifetime $c\tau$. In the top panel of Fig. 3, we demonstrate how Z' mass solutions showed in the color bar correlate with $\Delta a_\mu and \Delta a_e$. As expected, the behavior of m_Z' is very similar to g' in the top panel of Fig. 2. Herein, our 1 σ solutions are excluded for $m_Z' \approx 17$ MeV, the value satisfying the Atomki anomaly. Such Z' mass bound also puts an additional limit on g' and $\tilde{g}$, in addition to those already obtained rom the AMMs in Fig. 2. We also examine the Z' lifetime since it is crucial to explore potentially displaced signatures at the LHC. The plot at the bottom of Fig. 3 showcases the proper lifetime of Z' in milimeters over the mass range 16.7 MeV $\lesssim m_Z' \lesssim$ 18 MeV while the color bar indicates $\tilde{g}$. As mentioned in Ref. [36], for small values of $|\tilde{g}|$, the Z' lifetime becomes longer. Considering the $\tilde{g}$ solutions which fulfill all experimental conditions, the lifetime of the Z' should be $\sim 10^{-3}$ mm, which is not sufficient to produce a displaced detector signal.

A. Z' production at the LHC

Now, we will study the collider signatures of our light Z' boson in three different channels at the LHC: Drell-Yan (DY) and Z' pair production through both SM-like Higgs h_2 and exotic Higgs h_1 mediation, wherein we consider both fully leptonic and semi-leptonic final states.

1. *Drell-Yan*

At the LHC, the most favored process for a light Z' boson is the DY channel, where it can directly be generated via $q\bar{q}$ fusion in s-channel. In Fig. 4, we present the dilepton production cross section via our light Z' resonance. Although the corresponding Z' production and decay rates are always large for $m_{Z'} \approx 17$ MeV, the process is difficult to detect given the very light Z', implying very soft decay products. Hence, our Z' is not really constrained by present LHC data, so that all points presented in this plot (at $\sqrt{s} = 14$ TeV) are amenable to experimental investigation during Run 3. However, a more striking signature would be Z' pair production, to which we turn next.

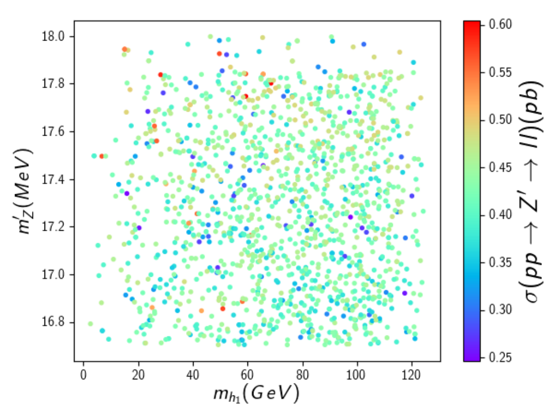

FIG. 4: Results for $\sigma(pp \to Z' \to ll)$ $(l = e, \mu)$ in terms of m_{h_1} vs $m_{Z'}$, for $\sqrt{s} = 14$ TeV.

2. *Z' Pair Production via SM-like Higgs Mediation*

As $m_{Z'} \ll m_{h_{1,2}}/2$, our light Z' boson can be pair produced via both Higgs bosons h_1 and h_2. Let us start with SM-like Higgs mediation. In Fig.5, we present the cross section of the ensuing four-lepton final state at $\sqrt{s} = 14$ TeV for the solutions satisfy all experimental bounds considered so far, with the additional requirement BR$(h_2 \to Z'Z' \to 4l) < 5 \times 10^{-6}$, following ATLAS [37] and CMS [38] results. The color bar shows the mass of the h_1. As can be seen, the rates for $\sigma(pp \to h_2 \to Z'Z' \to 4l)$ can be rather large, up to ≈ 0.1 fb, over a wide range of m_{h_1}, including very small values of the latter, which in turn call for studying h_1 mediation, our next section.

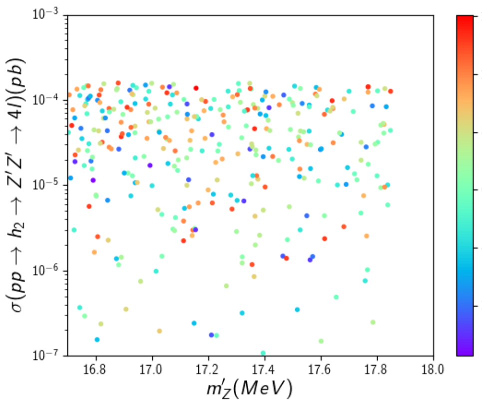

FIG. 5: Results for m_{h_1} in terms of $m_{Z'}$ vs $\sigma(pp \to h_2 \to Z'Z' \to 4l)$, for $\sqrt{s} = 14$ TeV.

3. Z' Pair Production via Exotic Higgs Mediation

In this final part, we investigate Z' pair production via the new exotic Higgs, h_1. Fig. 6 shows $\sigma(pp \to h_1 \to Z'Z' \to 4l)$ correlated to m_{h_1} as well as $m_{Z'}$, for the same parameter space considered in the previous plot (again, $\sqrt{s} = 14$ TeV). In this case, the four-lepton rate can be larger than 10×10^{-3} pb for a light h_1 while reaching 2×10^{-5} pb for m_{h_1} tending to m_{h_2}. Hence, the h_1 mediated process, depending on the m_{h_1} values, producing a Z' pair decaying into four-lepton final states, can actually the best way to access both the new Higgs and new gauge sectors of our scenario.

II. CONCLUSION

In summary, a rather simple theoretical framework, assuming a non-universally coupled (to fermions) Z' boson, with a mass of $O(10)$ MeV, emerging from a spontaneously broken $U(1)'$ group additional to the SM gauge symmetries, is able to explain several data anomalies currently existing at low energies while predicting a clear signal at high energies. Namely, the latter is a very clean process, potentially extractable at the upcoming Run 3 of the LHC, i.e., $pp \to h_i \to Z'Z' \to 4l$ $(l = e, \mu)$, where h_1 and h_2 are the new Higgs state associated to the additional gauge group and the SM-like one already discovered, respectively. Hence, a new 'golden channel' involving again four leptons in the final state could soon give access to both a new neutral Higgs and gauge boson.

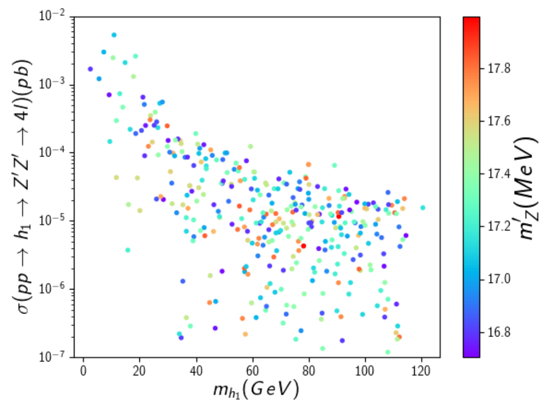

FIG. 6: Results for $m_{Z'}$ in terms of m_{h_1} vs $\sigma(pp \to h_1 \to Z'Z' \to 4l)$, for $\sqrt{s} = 14$ TeV.

ACKNOWLEDGEMENTS

SK is partially supported by the Science, Technology and Innovation Funding Authority (STDF) under Grant No. 37272. SM is supported in part through the NExT Institute and the STFC Consolidated Grant No. ST/L000296/1. The work of YH is supported by The Scientific and Technological Research Council of Turkey (TUBITAK) in the framework of the 2219-International Postdoctoral Research Fellowship Programme and by Balikesir University Scientific Research Projects with Grant No. BAP-2022/083.

[1] J. Gulyás, T. J. Ketel, A. J. Krasznahorkay, M. Csatlós, L. Csige, Z. Gácsi, M. Hunyadi, A. Krasznahorkay, A. Vitéz and T. G. Tornyi, Nucl. Instrum. Meth. A **808**, 21-28 (2016) [arXiv:1504.00489 [nucl-ex]].
[2] A. J. Krasznahorkay, M. Csatlós, L. Csige, Z. Gácsi, J. Gulyás, M. Hunyadi, T. J. Ketel, A. Krasznahorkay, I. Kuti and B. M. Nyakó, *et al.*, Phys. Rev. Lett. **116**, no.4, 042501 (2016) [arXiv:1504.01527 [nucl-ex]].
[3] N. J. Sas, A. J. Krasznahorkay, M. Csatlós, J. Gulyás, B. Kertész, A. Krasznahorkay, J. Molnár, I. Rajta, J. Timár and I. Vajda, *et al.*, [arXiv:2205.07744 [nucl-ex]].

[4] A. J. Krasznahorkay, M. Csatlós, L. Csige, J. Gulyás, T. J. Ketel, A. Krasznahorkay, I. Kuti, Á. Nagy, B. M. Nyakó and N. Sas, *et al.*, EPJ Web Conf. **142**, 01019 (2017).

[5] A. J. Krasznahorkay, M. Csatlós, L. Csige, J. Gulyás, M. Hunyadi, T. J. Ketel, A. Krasznahorkay, I. Kuti, Á. Nagy and B. M. Nyakó, *et al.*, PoS **BORMIO2017**, 036 (2017).

[6] A. J. Krasznahorkay, M. Csatlós, L. Csige, J. Gulyás, M. Hunyadi, T. J. Ketel, A. Krasznahorkay, I. Kuti, Á. Nagy and B. M. Nyakó, *et al.*, EPJ Web Conf. **137**, 08010 (2017).

[7] A. J. Krasznahorkay, M. Csatlós, L. Csige, Z. Gácsi, J. Gulyás, Á. Nagy, N. Sas, J. Timár, T. G. Tornyi and I. Vajda, *et al.*, J. Phys. Conf. Ser. **1056**, no.1, 012028 (2018).

[8] B. Barman, P. Ghosh, A. Ghoshal and L. Mukherjee, [arXiv:2112.12798 [hep-ph]].

[9] A. Bodas, R. Coy and S. J. D. King, Eur. Phys. J. C **81**, no.12, 1065 (2021) [arXiv:2102.07781 [hep-ph]].

[10] P. Fayet, Phys. Rev. D **103**, no.3, 035034 (2021) [arXiv:2010.04673 [hep-ph]].

[11] T. Nomura and P. Sanyal, JHEP **05**, 232 (2021) [arXiv:2010.04266 [hep-ph]].

[12] O. Seto and T. Shimomura, JHEP **04**, 025 (2021) [arXiv:2006.05497 [hep-ph]].

[13] C. Hati, J. Kriewald, J. Orloff and A. M. Teixeira, JHEP **07**, 235 (2020) [arXiv:2005.00028 [hep-ph]].

[14] B. Puliçe, Chin. J. Phys. **71**, 506-517 (2021) [arXiv:1911.10482 [hep-ph]].

[15] L. Delle Rose, S. Khalil and S. Moretti, Phys. Rev. D **96**, no.11, 115024 (2017) [arXiv:1704.03436 [hep-ph]].

[16] L. Delle Rose, S. Khalil, S. J. D. King, S. Moretti and A. M. Thabt, Phys. Rev. D **99**, no.5, 055022 (2019) [arXiv:1811.07953 [hep-ph]].

[17] J. P. Leveille, Nucl. Phys. B **137**, 63-76 (1978).

[18] J. Kozaczuk, D. E. Morrissey and S. R. Stroberg, Phys. Rev. D **95**, no.11, 115024 (2017) [arXiv:1612.01525 [hep-ph]].

[19] J. L. Feng, B. Fornal, I. Galon, S. Gardner, J. Smolinsky, T. M. P. Tait and P. Tanedo, Phys. Rev. Lett. **117**, no.7, 071803 (2016) [arXiv:1604.07411 [hep-ph]].

[20] W. Porod, Comput. Phys. Commun. **153**, 275-315 (2003) [arXiv:hep-ph/0301101 [hep-ph]].

[21] W. Porod and F. Staub, Comput. Phys. Commun. **183**, 2458-2469 (2012) [arXiv:1104.1573 [hep-ph]].

[22] J. Braathen, M. D. Goodsell and F. Staub, Eur. Phys. J. C **77**, no.11, 757 (2017) [arXiv:1706.05372 [hep-ph]].

[23] F. Staub, Comput. Phys. Commun. **185**, 1773-1790 (2014) [arXiv:1309.7223 [hep-ph]].

[24] F. Staub, Adv. High Energy Phys. **2015**, 840780 (2015) [arXiv:1503.04200 [hep-ph]].

[25] H. Davoudiasl and W. J. Marciano, Phys. Rev. D **98**, no.7, 075011 (2018) [arXiv:1806.10252 [hep-ph]].

[26] L. Morel, Z. Yao, P. Cladé and S. Guellati-Khélifa, Nature **588**, no.7836, 61-65 (2020).

[27] B. Abi *et al.* [Muon g-2], Phys. Rev. Lett. **126**, no.14, 141801 (2021) [arXiv:2104.03281 [hep-ex]].

[28] D. Banerjee *et al.* [NA64], Phys. Rev. Lett. **120**, no.23, 231802 (2018) [arXiv:1803.07748 [hep-ex]].

[29] S. Chatrchyan *et al.* [CMS], Phys. Lett. B **716**, 30-61 (2012) [arXiv:1207.7235 [hep-ex]].

[30] G. Aad *et al.* [ATLAS], Phys. Lett. B **716**, 1-29 (2012) [arXiv:1207.7214 [hep-ex]].

[31] Y. Amhis *et al.* [HFLAV], [arXiv:1207.1158 [hep-ex]].

[32] R. Aaij *et al.* [LHCb], Phys. Rev. Lett. **110**, no.2, 021801 (2013) [arXiv:1211.2674 [hep-ex]].

[33] D. Asner *et al.* [HFLAV], [arXiv:1010.1589 [hep-ex]].

[34] J. Erler, P. Langacker, S. Munir and E. Rojas, JHEP **08**, 017 (2009) [arXiv:0906.2435 [hep-ph]].

[35] A. Belyaev, N. D. Christensen and A. Pukhov, Comput. Phys. Commun. **184**, 1729-1769 (2013) [arXiv:1207.6082 [hep-ph]].

[36] T. Lagouri, Phys. Scripta **97**, no.2, 024001 (2022).

[37] G. Aad *et al.* [ATLAS], JHEP **03**, 041 (2022) [arXiv:2110.13673 [hep-ex]].

[38] A. Tumasyan *et al.* [CMS], Eur. Phys. J. C **82**, no.4, 290 (2022) [arXiv:2111.01299 [hep-ex]].